engineering proceedings

MDPI

Proceeding Paper

Integration of Deep Learning Methods into the Design of Microwave Transceiver Components for a 5G Mid-Band System †

Pedro Escudero-Villa *, Santiago Huebla-Huilca and Jenny Paredes-Fierro

Facultad de Ingeniería, Universidad Nacional de Chimborazo, Riobamba 060108, Ecuador; santiago.huebla@unach.edu.ec (S.H.-H.); patricia.paredes@unach.edu.ec (J.P.-F.)

* Correspondence: pedro.escudero@unach.edu.ec

† Presented at the 6th International Electronic Conference on Applied Sciences, 9–11 December 2025; Available online: https://sciforum.net/event/ASEC2025.

Abstract

This study evaluates the application of deep learning techniques to the design of a microwave transmitter–receiver system operating in the 5G mid-band. The proposed architecture consists of four stages—signal generation, amplification, mixing, and filtering—each initially designed using conventional microwave methods and subsequently integrated into a complete transceiver. Simulation data were generated and component-specific convolutional neural networks (CNNs) were implemented in Python using TensorFlow/Keras. Across all models, an average error reduction exceeding 90% was achieved, with most networks converging after the third training cycle. System-level integration shows that the baseline design achieved a transmitted power of −32.637 dBm and a gain of 1.116 dB, while the deep learning-based design yielded −33.912 dBm and 0.738 dB. Additional analysis of S-parameters confirms acceptable impedance matching and a frequency response of around 3.5 GHz. These results illustrate that deep learning provides an effective complementary methodology for multi-component microwave system modeling and optimization in 5G applications.

Keywords: deep learning; convolutional neural networks; microwave systems; 5G NR mid-band; transceiver design

1. Introduction

Modern communication systems rely heavily on radiofrequency (RF) and microwave technologies to support high-speed data transmission, broad bandwidth, and low-latency services essential for fifth-generation (5G) networks and emerging applications. These technologies enable the operation of advanced transmitters, receivers, filters, amplifiers, and frequency converters, all of which must perform reliably under increasingly demanding performance specifications [1]. As 5G services expand across sub-6 GHz bands—including the mid-band segment between 400 MHz and 7 GHz—designers face new challenges in achieving efficient, compact, and highly linear microwave systems. Conventional design methodologies, based on analytical models, electromagnetic simulation, and iterative prototyping, remain fundamental; however, the complexity of modern RF chains has intensified the need for complementary techniques capable of reducing design time and enhancing system adaptability.

Deep learning (DL), offers an effective alternative for capturing nonlinear patterns, modeling high-dimensional relationships, and accelerating engineering workflows [2,3].

Check for updates

Academic Editor: Alessandro Lo Schiavo

Published: 30 March 2026

Copyright: © 2026 by the authors. Licensee MDPI, Basel, Switzerland. This article is an open access article distributed under the terms and conditions of the Creative Commons Attribution (CC BY) license.

Convolutional and deep architectures excel at learning complex input–output mappings in microwave structures, which has encouraged their adoption in RF device modeling. Prior studies have demonstrated the usefulness of DL for designing microstrip filters [4], nonlinear microwave components [5], parametric structures [6], and fast frequency-domain simulations [7]. Deep learning has also been applied to communications, enabling intelligent filtering, adaptive detection, and resource optimization in wireless systems [8–10]. These developments show that DL can complement traditional microwave design by reducing the computational cost and handling multidimensional parameter spaces more efficiently. Despite these advances, a key problem persists: most existing research focuses on individual RF or microwave components, such as filters, amplifiers, or antennas [9,11,12].

Studies rarely explore the holistic modeling and design of an entire transmitter–receiver (TX–RX) chain, where multiple nonlinear and linear components interact [13–15]. This gap limits our understanding of whether neural networks can generalize beyond isolated device behavior and accurately replicate the operation of a complete microwave communication system [15]. Traditional electromagnetic simulation tools such as ADS and HFSS provide highly detailed modeling but require considerable computational resources, long simulation times, and expert configuration, making iterative system-level design increasingly demanding [16]. A data-driven alternative capable of approximating the behavior of multiple RF stages can significantly streamline design cycles and support rapid prototyping for 5G systems.

To address the increasing complexity of microwave system design in 5G applications, this study explores the use of deep learning as a data-driven alternative for modeling and designing a microwave transmitter–receiver operating in the mid-band. Deep neural networks are employed to approximate the behavior of essential RF components, including filters, amplifiers, mixers, and low-pass stages, and to integrate their predicted parameters into a complete communication system. Component-level models are trained using simulation data and subsequently validated through system-level integration. A performance evaluation is conducted using key indicators such as gain, scattering parameters, harmonic response, and error reduction after training.

2. Methodology

2.1. System Definition and Design Constraints

The proposed microwave transmitter–receiver system was designed to operate in the 5G mid-band, targeting a carrier frequency of 3.5 GHz and a 100 MHz baseband bandwidth, in accordance with the 5G NR FR1 specification. The system architecture comprised four cascaded stages (Figure 1): signal generation, amplification, frequency mixing, and filtering. These stages were configured for up-conversion in the transmitter and down-conversion in the receiver, enabling end-to-end signal recovery.

The same components were reused in both transmission and reception paths, with only configuration changes in the mixer and filter stages. This design choice enabled a direct comparison between base and deep learning-assisted implementations while minimizing architectural variability.

2.2. Conventional Base Design and ADS Simulation

A reference transmitter–receiver system was first designed using analytical equations and validated through Advanced Design System (ADS, 30-day trial license) simulations (see Supplementary Materials). Each component was designed and verified individually before system integration (Figure 2). The bandpass filter was implemented using coupled microstrip lines designed for a center frequency of 3.5 GHz and a Chebyshev response. The microwave amplifier was designed to ensure unconditional stability and maximum gain at

the target frequency. The RF mixer was implemented using a hybrid coupler and Schottky diodes, followed by a low-pass filter to extract the baseband signal after down-conversion. Each component was simulated independently to verify frequency response, gain, and harmonic behavior prior to integration.

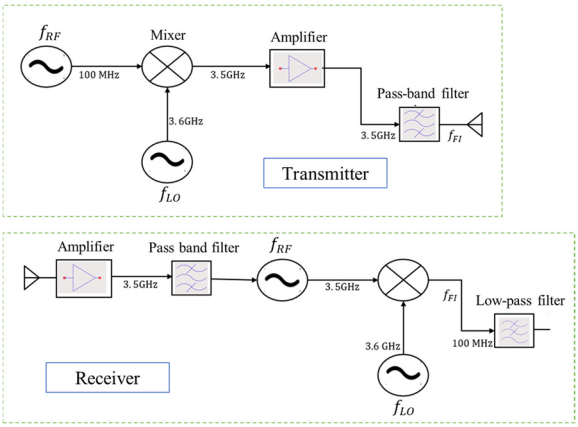


Figure 1. Block diagram of the four-stage transmitter–receiver system.

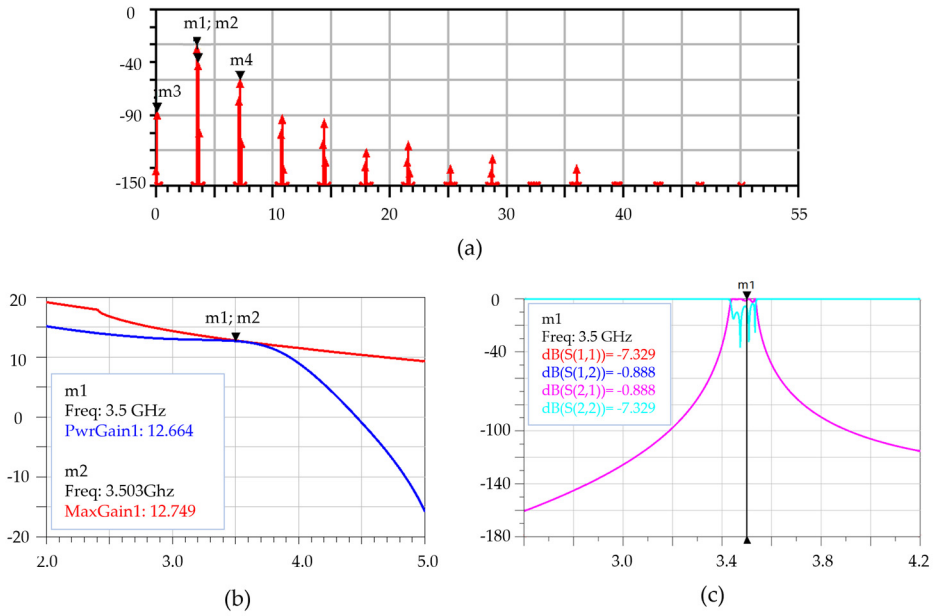


Figure 2. Harmonic balance analysis of the mixer (**a**), maximum available gain versus simulated gain (**b**), and S-parameters of the bandpass filter (**c**). Frequency in GHz is shown on the X-axis for all subfigures.

After individual validation, the components were integrated into complete transmitter and receiver schematics.

2.3. Dataset Generation for Neural Network Training

To enable data-driven modeling, datasets were generated using MATLAB (R2025a, 30-day trial version) scripts implementing the analytical design equations of each component. Design variables such as frequency, impedance, ripple, bandwidth, and filter order were systematically varied within predefined ranges to generate representative input–output mappings (Table 1). Each component was treated independently, resulting in four datasets, one per stage. The generated data represent physically meaningful solutions that satisfy microwave design constraints. The final dataset consisted of 24,232 samples, distributed across the four components.

Table 1. Input/output variables used for neural network training of microwave components.

Component	Input Variables (Range)	Output Variables
Bandpass Filter	Bandwidth (0.1–10%), Ripple (0.5, 3.0 dB), Impedance (20–50 Ω)	Even/odd impedances of coupled-line sections (1–6)
Microwave Amplifier	Frequency (0.1–10 GHz)	Source and load matching network dimensions (transmission line and stub)
RF Mixer and LPF	Cutoff frequency (1–5 GHz), Impedance (20–100 Ω)	Hybrid coupler line impedances (lines 1–4); LPF components (C1, L2, C3, L4, C5)

2.4. Neural Network Configuration and Training Procedure

Four independent neural networks were implemented using Python 3.13.2 and trained using the generated datasets. Each network was tailored to the dimensionality and characteristics of its corresponding component (see Supplementary Materials). The architectures combined convolutional layers with sequential organization, enabling the efficient extraction of relevant design features. Across all networks, a total of 338 layers were distributed among input, hidden, and output layers. Training was performed using mean absolute error (MAE) and mean squared error (MSE) as evaluation metrics (Figure 3). Each network underwent five independent training runs to assess convergence stability and robustness. Training progress was monitored by tracking the evolution of MAE and MSE across epochs.

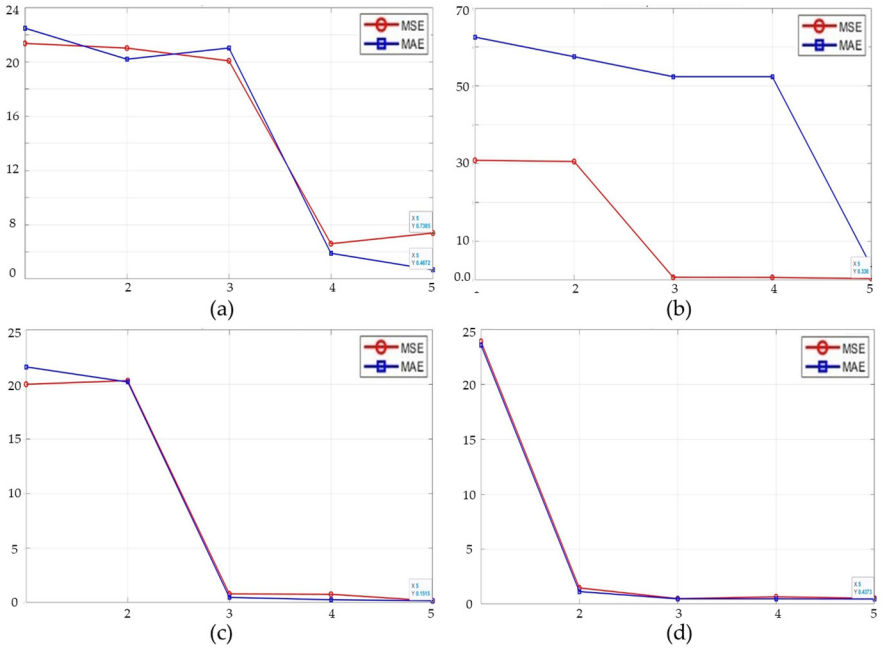


Figure 3. MAE and MSE evolutions to (**a**) Network 1, (**b**) Network 2, (**c**) Network 3, and (**d**) Network 4. Percentage values for the Y-axis, and training iterations for the X-axis.

To summarize training effectiveness, the percentage reduction of MAE and MSE was computed for each network (Figure 4).

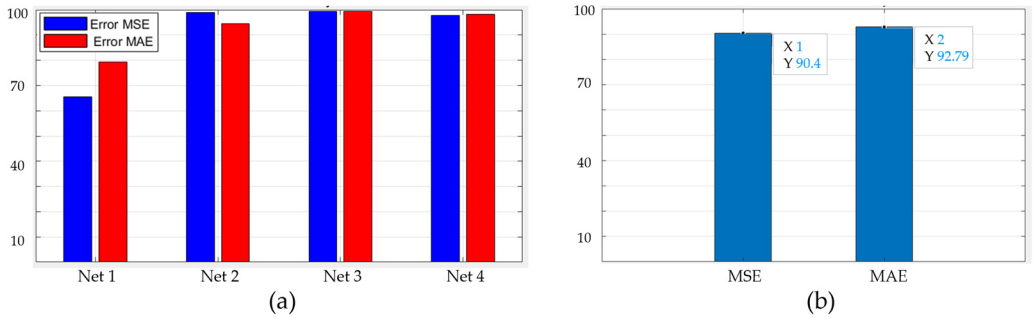


Figure 4. (**a**) Percentage error reduction per network; (**b**) average MAE and MSE reductions.

2.5. Deep Learning-Based System Integration

After training, the predicted component parameters were exported and used to reconstruct the transmitter and receiver in ADS. The same simulation settings and analysis tools used for the base design were applied to the deep learning-based system, ensuring direct comparability. System-level simulations included harmonic balance analysis, time-domain signal inspection, and frequency-domain evaluation at key nodes of the transmitter and receiver.

3. Results and Discussion

3.1. Training Performance Analysis

The neural networks initially produced high error values due to the complexity of the input–output relationships between design parameters and microwave component behavior. As training progressed, both MAE and MSE decreased consistently across successive iterations. In the final training run, all networks achieved an average error reduction exceeding 90%, indicating stable convergence and reliable learning of the component design relationships. The results show that the generated datasets captured the relevant parameter dependencies for each component and that the selected network configurations were capable of approximating the microwave responses derived from analytical design equations.

The training datasets were generated using MATLAB scripts based on microwave design formulas and validated through ADS simulations. Although simulation-based datasets allow the controlled generation of large numbers of samples, they do not include non-ideal hardware effects such as manufacturing tolerances, temperature variation, or device aging. Consequently, the current model represents the ideal behavior of the components under nominal conditions.

3.2. System-Level Signal Validation

System-level simulations confirm correct operation of the transmitter and receiver stages (Figure 5). In the transmitter, the 100 MHz baseband signal is modulated and up-converted to a carrier centered near 3.5 GHz. At the receiver, the high-frequency signal is down-converted and filtered, allowing the recovery of the baseband waveform. Frequency-domain analysis shows that the spectral translation occurs at the expected frequencies, indicating that the learned parameters maintain correct signal propagation across the cascaded stages.

This validation demonstrates that component-level models trained using deep learning can be integrated into a complete transmitter–receiver architecture without altering the expected signal flow or frequency translation behavior.

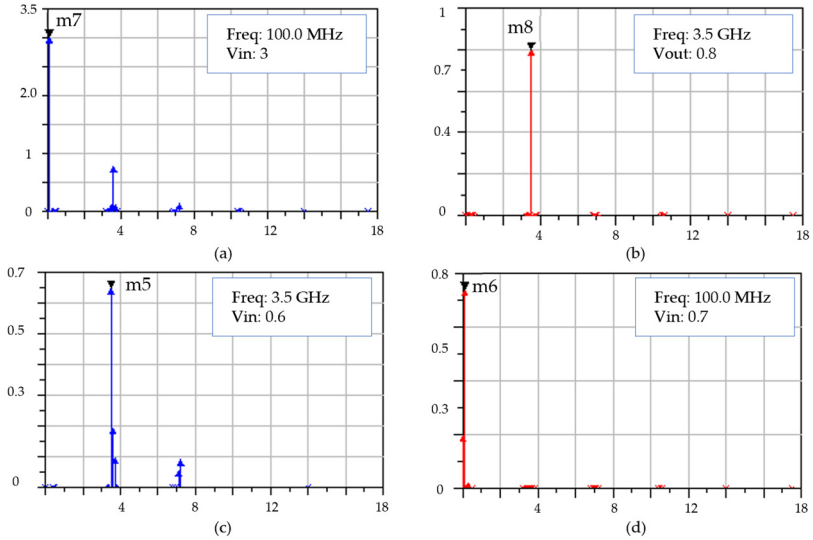


Figure 5. Frequency-domain signals for the transmitter input (**a**) and output (**b**), and for the receiver input (**c**) and output (**d**). Vin in volts for the Y-axis, and frequency in GHz for the X-axis.

3.3. Power and Gain Comparison

A quantitative comparison between the baseline analytical design and the deep learning-based implementation shows small differences in the system performance (Table 2). The baseline design achieved an output power of −32.637 dBm with a gain of 1.116 dB, whereas the deep learning-based configuration produced −33.912 dBm and 0.738 dB. The resulting gain difference of approximately 0.37 dB indicates that the parameters predicted by the neural networks produce system responses close to the reference design.

Table 2. Power and gain values: base design vs. deep learning.

	Base Design	**Deep Learning**
Input	−33.753 dBm	−33.652 dBm
Output	−32.637 dBm	−33.912 dBm
Gain	1.116 dB	0.738 dB

The current evaluation focuses on metrics directly related to component modeling and signal propagation, including output power, gain, S-parameters, and harmonic balance response. While these metrics provide insight into system functionality, additional performance indicators commonly used in communication systems—such as P1dB compression point, third-order intercept point (IP3), harmonic distortion, intermodulation distortion, error vector magnitude (EVM), and signal-to-noise ratio (SNR)—could further characterize system behavior under practical operating conditions.

The results demonstrate that component-level deep learning models can be successfully integrated into a complete microwave transmitter–receiver system without compromising the system-level performance (Figure 6). The small gain deviation and accurate baseband recovery indicate that the neural networks effectively capture the nonlinear interactions between design variables and component behavior. From an engineering perspective, this approach reduces design iteration time during early-stage system exploration. Instead of repeatedly tuning analytical models and simulations, trained networks can estimate component parameters that meet system requirements. The current validation relies on simulation data; however, the methodology can be extended to experimental characterization and hardware-in-the-loop testing. Future work will incorporate measured data, manufacturing tolerances, and adaptive training to improve robustness and generalization.

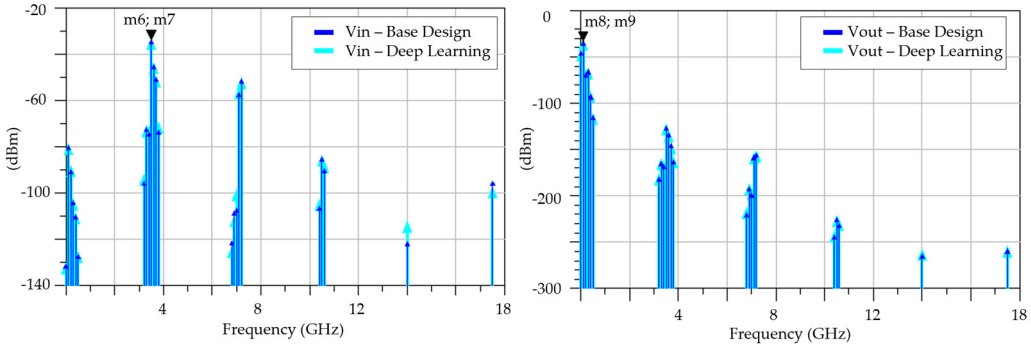


Figure 6. (**a**) Input and (**b**) output power comparison at the receiver.

4. Conclusions

This work demonstrates that while prior research has applied deep learning models to the design and optimization of individual microwave devices, their scope has generally remained limited to isolated components. In contrast, the present work integrates multiple microwave devices into a complete communication system, providing a more holistic perspective. A deep neural network architecture combining convolutional and sequential models was implemented, proving effective in capturing the complex input–output relationships of the system. To enable robust learning, a base system composed of four functional components and four neural networks was designed. Training was performed using 24,232 data samples and a total of 338 layers distributed across input, hidden, and output layers. A performance evaluation based on MAE and MSE metrics showed error reductions exceeding 90%, confirming strong model convergence and accurate pattern learning. A system-level evaluation further revealed a transmission frequency response of 3.5 GHz and a recovered signal bandwidth of 100 MHz. The receiver output power of −32.912 dBm and a gain of 0.738 dB, with only a 0.37 dB deviation from design values, indicate minimal losses. Overall, the results confirm that the proposed system operates efficiently and supports reliable transmission in 5G environments. Future work will incorporate measured data from fabricated microwave structures and additional boundary-case samples, including impedance mismatch and extreme operating conditions, to further evaluate model robustness and generalization.

Supplementary Materials: The following supporting information can be downloaded at: https://www.mdpi.com/article/10.3390/engproc2026124095/s1, Figure S1: Transsmiter; Figure S2: Receptor; Figure S3: Input output signals for each individual component simulated; Table S1: Neural Network Architecture 1 (Filter); Table S2: Neural Network Architecture 2 (Filter); Table S3: Neural Network Architecture 3 (Directional Coupler); Table S4: Neural Network Architecture 4 (Directional Coupler);

Author Contributions: Conceptualization, P.E.-V. and S.H.-H.; methodology, P.E.-V. and S.H.-H.; software, S.H.-H.; validation, P.E.-V.; formal analysis, J.P.-F. and P.E.-V.; investigation, S.H.-H., P.E.-V., and J.P.-F.; resources, P.E.-V.; data curation, S.H.-H. and J.P.-F.; writing—original draft preparation, P.E.-V. and J.P.-F.; writing—review and editing, P.E.-V. and J.P.-F.; visualization, S.H.-H.; supervision, P.E.-V.; project administration, P.E.-V.; funding acquisition, P.E.-V. and S.H.-H. All authors have read and agreed to the published version of the manuscript.

Funding: This work was partially supported by funding from Vicerrectorado de Investigación, Vinculación y Posgrado (VIVP-Project No. 358-DIR.INV-GI-UNACH-2025), Universidad Nacional de Chimborazo, Ecuador.

Institutional Review Board Statement: Not applicable.

Informed Consent Statement: Not applicable.

Data Availability Statement: The original contributions presented in this study are included in the article. Further inquiries can be directed to the corresponding authors.

Conflicts of Interest: The authors declare no conflicts of interest.

References

1. Sagar, M.S.I.; Ouassal, H.; Omi, A.I.; Wisniewska, A.; Jalajamony, H.M.; Fernandez, R.E.; Sekhar, P.K. Application of Machine Learning in Electromagnetics: Mini-Review. *Electronics* **2021**, *10*, 2752. [CrossRef]
2. Razzaq, K.; Shah, M. Machine Learning and Deep Learning Paradigms: From Techniques to Practical Applications and Research Frontiers. *Computers* **2025**, *14*, 93. [CrossRef]
3. Escudero, P.; Alcocer, W.; Paredes, J. Recurrent Neural Networks and ARIMA Models for Euro/Dollar Exchange Rate Forecasting. *Appl. Sci.* **2021**, *11*, 5658. [CrossRef]
4. Zhang, C.; Jin, J.; Na, W.; Zhang, Q.-J.; Yu, M. Multivalued Neural Network Inverse Modeling and Applications to Microwave Filters. *IEEE Trans. Microw. Theory Tech.* **2018**, *66*, 3781–3797. [CrossRef]
5. Liu, W.; Na, W.; Zhu, L.; Ma, J.; Zhang, Q.-J. A Wiener-Type Dynamic Neural Network Approach to the Modeling of Nonlinear Microwave Devices. *IEEE Trans. Microw. Theory Tech.* **2017**, *65*, 2043–2062. [CrossRef]
6. Zhang, W.; Feng, F.; Liu, W.; Yan, S.; Zhang, J.; Jin, J.; Zhang, Q.-J. Advanced Parallel Space-Mapping-Based Multiphysics Optimization for High-Power Microwave Filters. *IEEE Trans. Microw. Theory Tech.* **2021**, *69*, 2470–2484. [CrossRef]
7. Mattucci, E.; Feng, L.; Benner, P.; Romano, D.; Antonini, G. *Fast Frequency-Domain Analysis for Parametric Electromagnetic Models Using Deep Learning*; IEEE: New York, NY, USA, 2023; pp. 1–3.
8. Ma, J.; Dang, S.; Li, P.; Watkins, G.; Morris, K.; Beach, M. Transfer Learning for the Behavior Prediction of Microwave Structures. *IEEE Microw. Wirel. Technol. Lett.* **2023**, *33*, 126–129. [CrossRef]
9. Sun, Z.; Li, J.; Fan, J. Convolutional Neural Filtering for Intelligent Communications Signal Processing in Harsh Environments. *IEEE Access* **2021**, *9*, 8212–8219. [CrossRef]
10. Marseet, A.; Sahin, F. *Application of Complex-Valued Convolutional Neural Network for Next Generation Wireless Networks*; IEEE: New York, NY, USA, 2017; pp. 1–5.
11. Peik, S.E.; Coutts, G.; Mansour, R.R. *Application of Neural Networks in Microwave Circuit Modelling*; IEEE: New York, NY, USA, 1998; Volume 2, pp. 928–931.
12. Jin, J.; Zhang, C.; Feng, F.; Na, W.; Ma, J.; Zhang, Q.-J. Deep Neural Network Technique for High-Dimensional Microwave Modeling and Applications to Parameter Extraction of Microwave Filters. *IEEE Trans. Microw. Theory Tech.* **2019**, *67*, 4140–4155. [CrossRef]
13. Lancho, A.; Weiss, A.; Lee, G.C.F.; Jayashankar, T.; Kurien, B.G.; Polyanskiy, Y.; Wornell, G.W. RF Challenge: The Data-Driven Radio Frequency Signal Separation Challenge. *IEEE Open J. Commun. Soc.* **2025**, *6*, 4083–4100. [CrossRef]
14. Doha, S.R.; Abdelhadi, A. Deep Learning in Wireless Communication Receivers: A Survey. *IEEE Access* **2025**, *13*, 113586–113605. [CrossRef]
15. Zhang, Y.; Wang, X.; Wang, Y.; Yan, N.; Feng, L.; Zhang, L. Accurate Design of Microwave Filter Based on Surrogate Model-Assisted Evolutionary Algorithm. *Electronics* **2022**, *11*, 3705. [CrossRef]
16. Sahu, K.C.; Koziel, S.; Pietrenko-Dabrowska, A. Surrogate Modeling of Passive Microwave Circuits Using Recurrent Neural Networks and Domain Confinement. *Sci. Rep.* **2025**, *15*, 13322. [CrossRef] [PubMed]

Disclaimer/Publisher's Note: The statements, opinions and data contained in all publications are solely those of the individual author(s) and contributor(s) and not of MDPI and/or the editor(s). MDPI and/or the editor(s) disclaim responsibility for any injury to people or property resulting from any ideas, methods, instructions or products referred to in the content.